Complete Hydraulic Fracture Modeling of the Full Montney

B. Doug Bearinger
Completions Geoscience

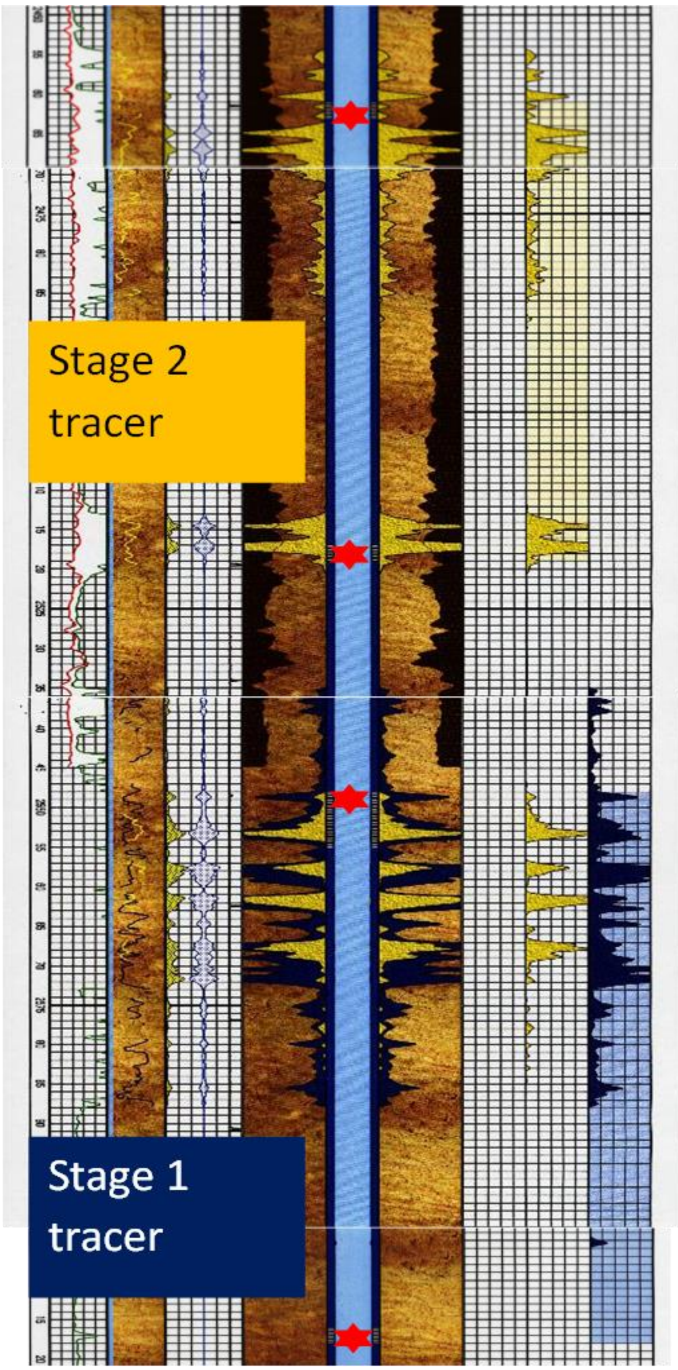

Figure 1: Proppant tracer log

Summary

The Montney of northeast British Columbia, Canada (NEBC) presents some challenges to hydraulic fracture modeling. Planar Hydraulic (induced) Fracture models do not account for most of the fluid pumped. This casts doubt on their ability to assess optimal well spacing, stratigraphic positioning, induced seismicity and wellbore deformation. Fracturing surveillance measurements show that fluid enters fault and fold structures, through fractures and bedding planes. A Discrete Fracture Network (DFN) tool (FracMan®) was used to trace where the fracturing fluid goes, using a comprehensive model of discontinuities in a well described geomechanical model within a well constrained stress field. Both vertical and horizontal wells in the Farrell Creek (Altares) area provide a rich engineering and geoscience dataset for this study.

The Full Montney Section

Vertical wells provide the logs, cores, and hydraulic fracture data to build the geomechanical model and include the essential discontinuities that can accept fracturing fluid. Even though the normal stress on the bedding planes (vertical stress) is about 10 MPa higher than the normal stress on an induced fracture (minimum horizontal stress), bedding planes are clearly inflated as evidenced by a proppant tracer log and frequent shear displacements, as observed in multiple reported casing deformations (McLellan 2014).

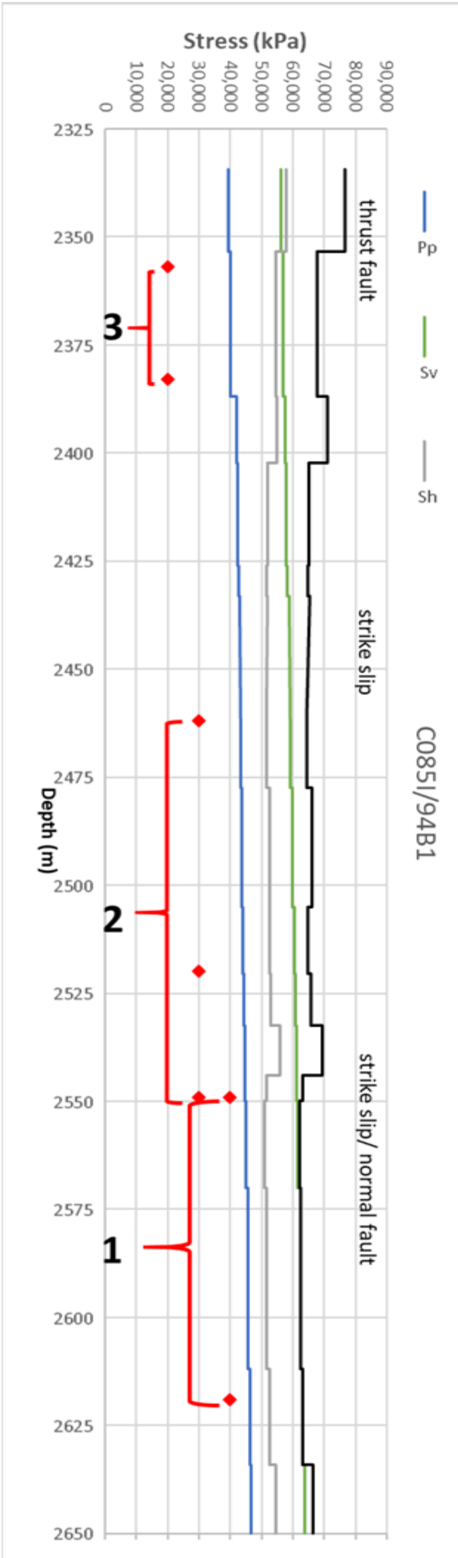

Figure 2: Gridded Stress Profile

Keneti (2011) measured mechanical properties of Montney samples.. The presence of bedding planes with low tensile strength (0.7-2.8 MPa) versus a high intact tensile strength parallel to bedding (6-15.3 MPa) makes opening bedding planes relatively easy with pumping pressures higher than the vertical stress (ISIP ~ 3.5 MPa > Sv). Elastic anisotropy also favors inflation of bedding planes. In core tests the Montney is about 35% stiffer in the horizontal direction than in the vertical direction.

This study focusses on a vertical well with 3 hydraulic stimulations in the Lower Montney, Upper Montney and Doig Formations of the Altares field of NEBC (Fig. 2).

The lower perf cluster (red diamonds) of the Lower Montney Stage 1 had little inflow during underbalanced perforation. After the stimulation, the sand top in the well was tagged above the lower perforations. No proppant tracer was detected at the lower perforations and it is likely that little fluid entered those perforations during the stimulation. For Stage two in the Upper Montney two perf clusters were added and a sand plug was set above the lower perforations in the Lower Montney. The stage 2 proppant tracer (yellow in Fig. 1) indicates that 3 perforation clusters received proppant.

For modeling purposes, dynamic elastic properties were computed from the dipole sonic logs and converted to static using the factors determined by Song (2012). From core data, the Biot's poro-elastic parameter and the horizontal versus vertical elastic modulus anisotropy were determined to be 0.65 and 1.36 respectively. These were upscaled to a 3D grid layered by petrophysical property clusters as determined in Davey (2012).

The 3D stress model uses poro-elastic, anisotropic modified Eaton equations and solves for tectonic strains to match DFIT results from area wells. Overburden thickness varies the stresses across the model. The stress model was validated by borehole breakouts and drilling induced tensile fractures interpreted on a micro-resistivity image log. Both thermal and equivalent circulating density effects were included in the borehole stress analyses.

Conductive bedding planes (left, green) and natural fractures were interpreted from the image log. The natural fractures intersecting the well are bed bound (Fig. 3). Active bedding planes were interpreted from the larger proppant tracer peaks and are shown as yellow. Some correspond to conductive bedding planes, others at the boundary of resistive/stiff beds and at changes in bedding texture.

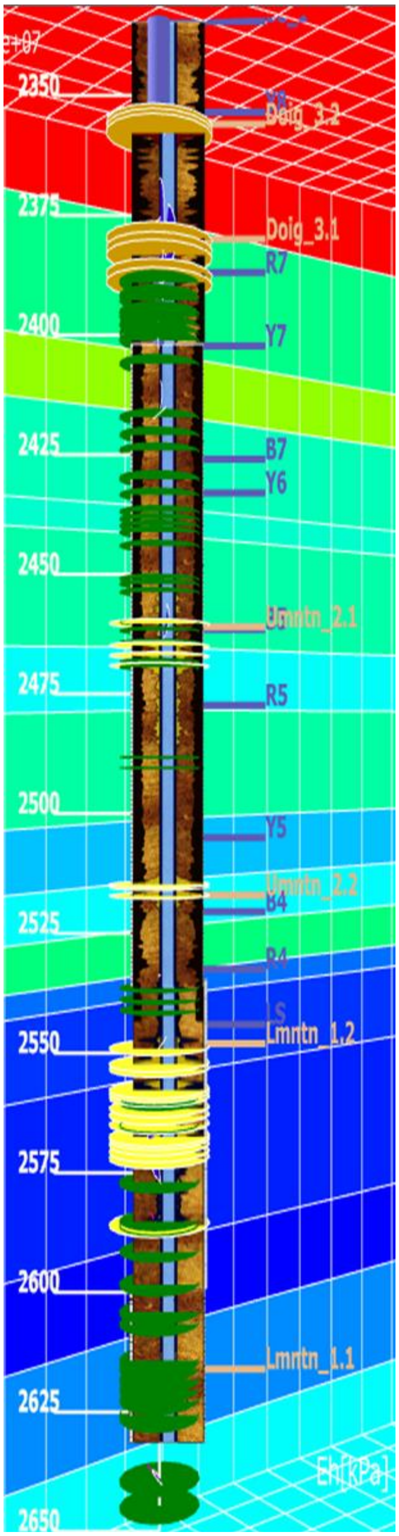

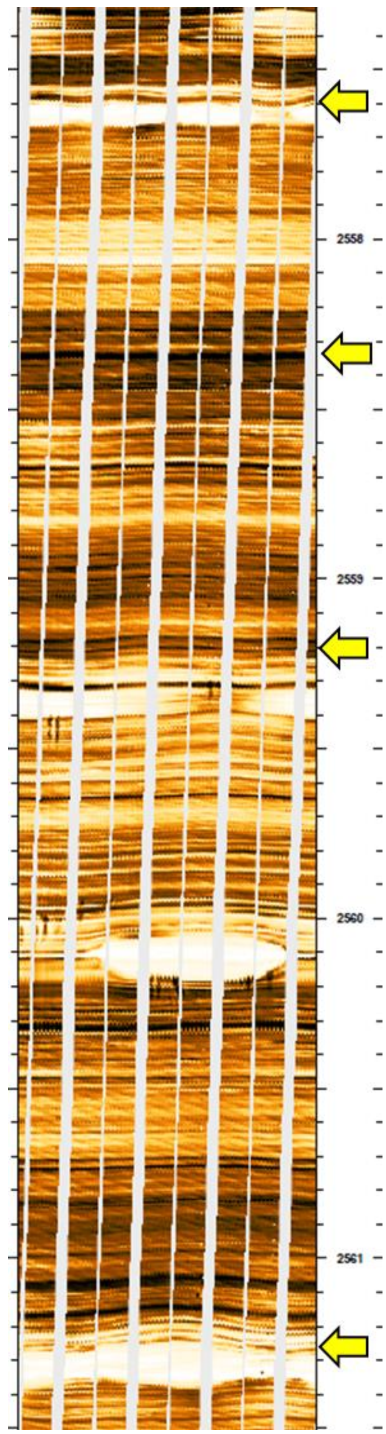

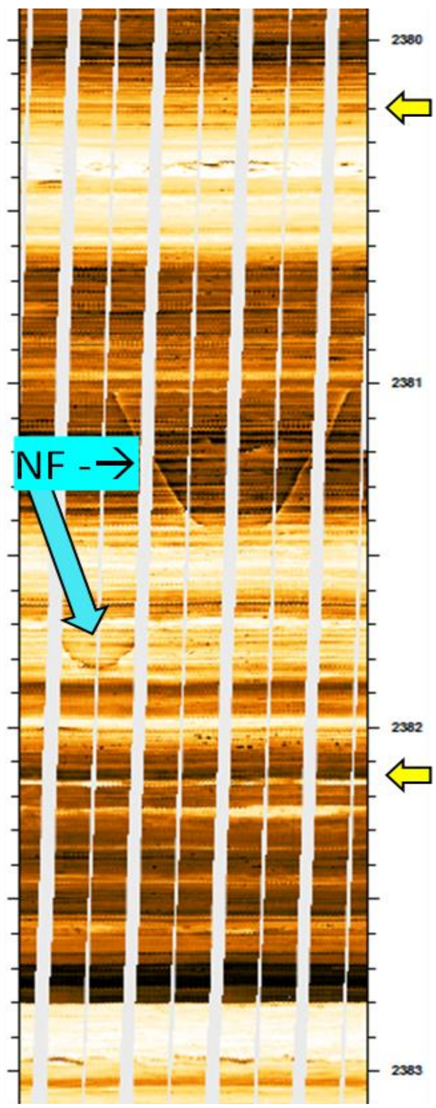

Figure 3: Left-Interpreted beds shown against the tracer log, center and right -imaged examples of traced beds.

In a hydraulic fracturing model, the volume of fluid, mass of proppant and the entry points are well known. The question to be answered is where do the fluid and proppant go? To enable the inclusion of important geological features and to keep run times small, FracMan replaces some of the complex physics with a rule based (heuristic) approach. The initial fracture at the wellbore can be a new tensile fracture or be selected from intersecting natural fractures. The algorithm determines where the fluid goes as natural fractures are encountered by the invading fluid by weighting the importance of critical properties, namely connection level (how many fractures connect it back to the induced fracture), transmissivity and fracture orientation. Growth and dilation of the induced fracture and inflation of natural fractures are dependent on net pressure, natural fracture storage (initial storage aperture), distance of fluid invasion and matrix elasticity. A form of the pressure width equation is used to calculate fracture dilation.

For this analysis, the geologic grid has mechanical layers from 7 to 42m thick, uses 20 x 20m grid cells and 10m finite elements for fracture discretization. A stage runs in about 2 seconds as the Discrete Fracture Network is quite small in this model and the rules-based approach is computationally very fast.

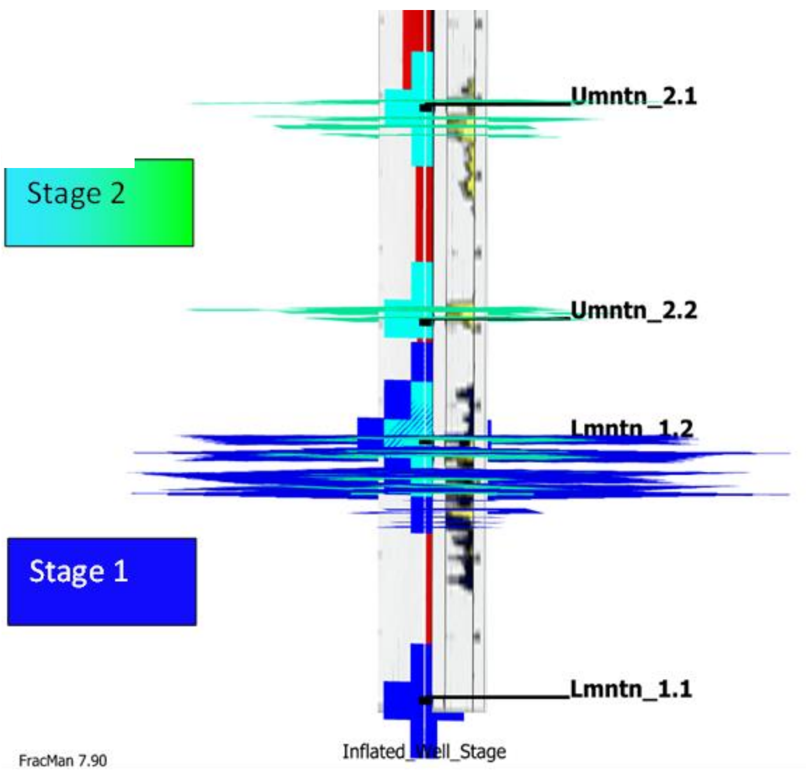

The Montney stages 1&2 results agree with the tracers (dark blue=stage1, yellow=stage2)

The upper perforations in the Lower Montney have a larger volume from Stage1 and a stronger stage 1 tracer amplitude.

The width of the red band behind the fractures represents the cumulative flow contribution from production logging.

Figure 4: Modeled hydraulic fracturing stages 1 & 2 with shaded tracer & cumulative production logs.

Stage 1 was run with the lower two perforation clusters open Poor inflow during perforating and lack of proppant tracers suggests that the lower perforation may have not been effective. The Hydraulic Fracture simulation suggests that they would have taken some fluid and production logging indicates that the lower perforations are productive. The 1.1 MPa higher minimum horizontal stress at the lower perforations, limits the dilation and growth of the induced fracture (Fig. 5).

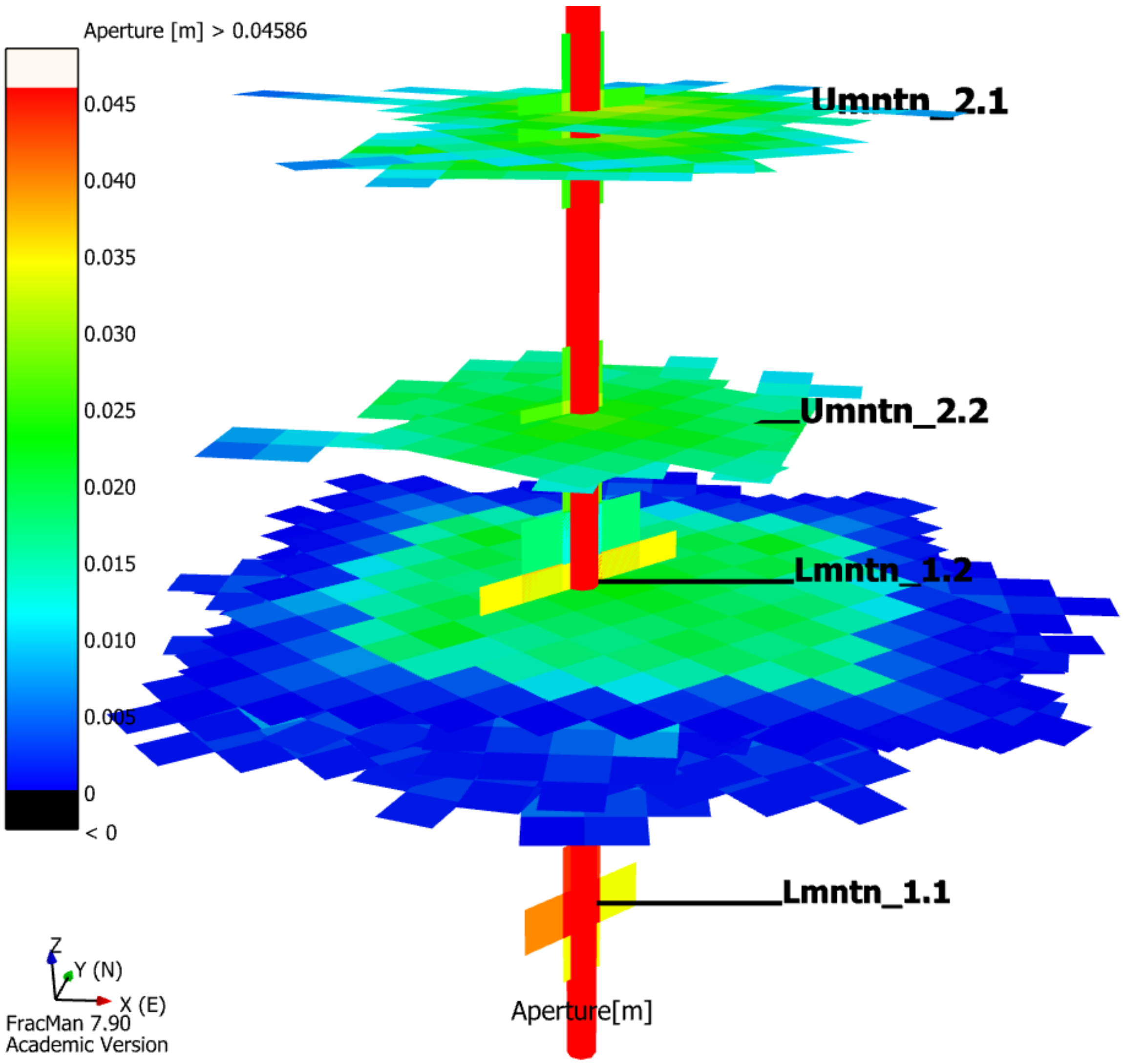

Figure 5: Modeled dilated fracture apertures of stages 1 & 2.

The simulations indicate that only 6.5% of the fluid occupies the induced fracture in Stage 1 with only 1.3% of the fracture surface area. In Stage 2, 3% of the fluid is used to grow the induced fractures, with 97% going into the bedding planes. Pressure fall-off is modelled with a square root of distance decay of net pressure (Figure 6).

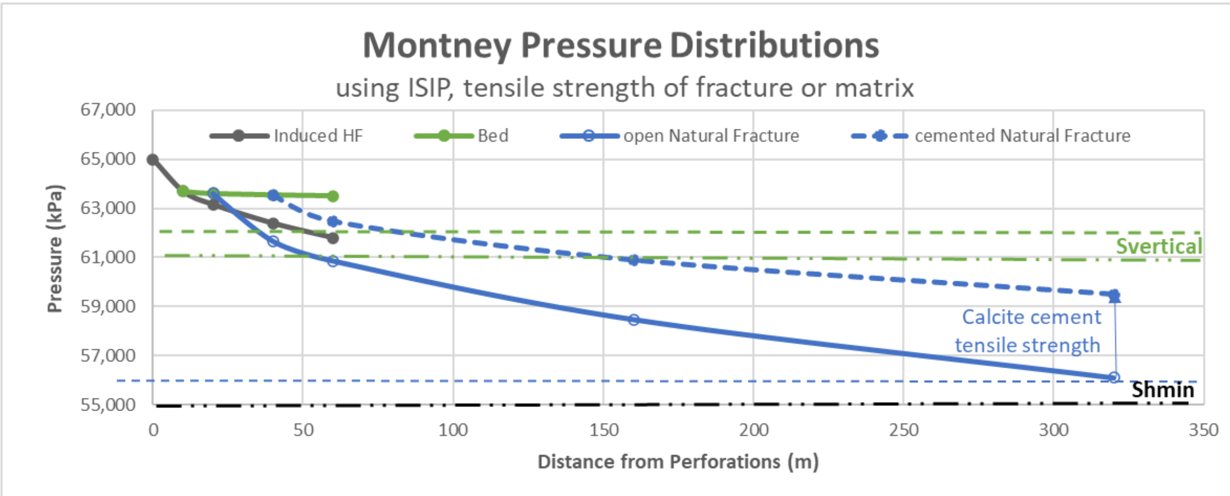

Figure 6: Conceptual view of pressure fall off away from the treating well from Initial Shut-in Pressure (ISIP) at the perforations to the acting normal stress + tensile strength at the tip of inflation of each element. The induced fracture feeds into a bedding plane at 10m from the perforations, an open natural fracture at 20 m and a calcite cemented natural fracture at 40 m distance.

Stages 1 & 2 were rerun without bedding planes as conventional planar fracturing simulations using a Carter Leak-off co-efficient of 3 (Fig. 7). The induced fractures have a greater vertical extent than the proppant tracer and do not match the tracer log amplitudes.

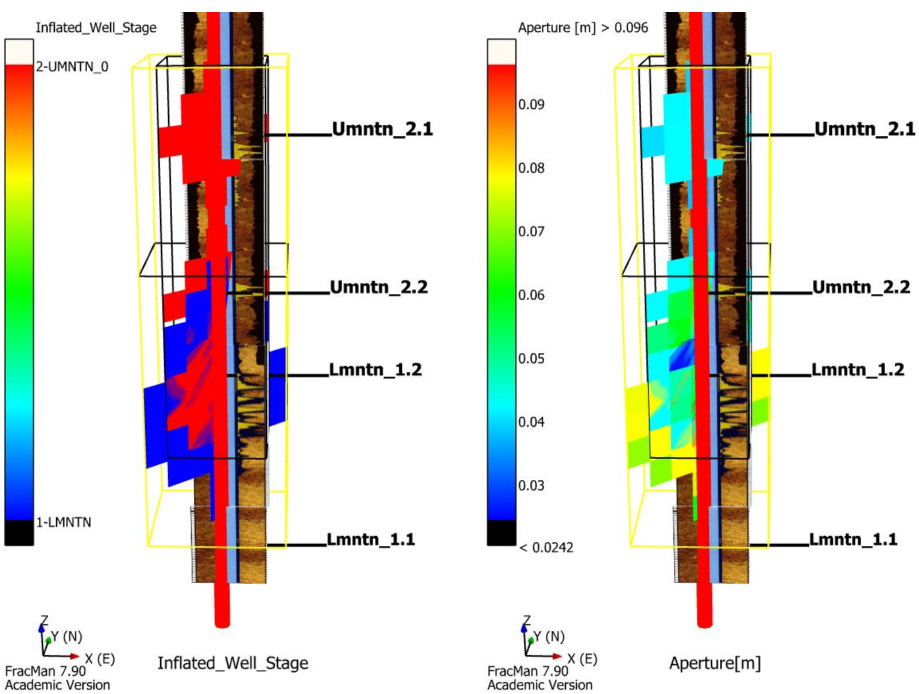

Figure 7: Simulated Induced fractures without activated bedding planes. Left-stage number, right- apertures.

The induced fractures took 20.9% and 15.7% of the pumped fluid with the remainder as leak-off. They had about 2-3 times the surface area as compared to induced fractures in the simulations that included bedding planes. Compared to simple planar induced fractures, the DFN simulations that include bedding planes generate 14-32 times the fracture surface area. Even with reduced vertical matrix perm, the bedding planes could have significant impact on production.

A 3rd stage in the Doig was simulated (Figure 8). The Induced fractures took only 0.5% of the fluid. This result cannot be matched with an induced fracture with leak-off. If the stress model is pushed into a thrust fault stress regime, a planar fracture model could generate a horizontal fracture at each perforation cluster but not match the downward growth of the lower fracture and the multiple tracer peaks as shown in the inset.

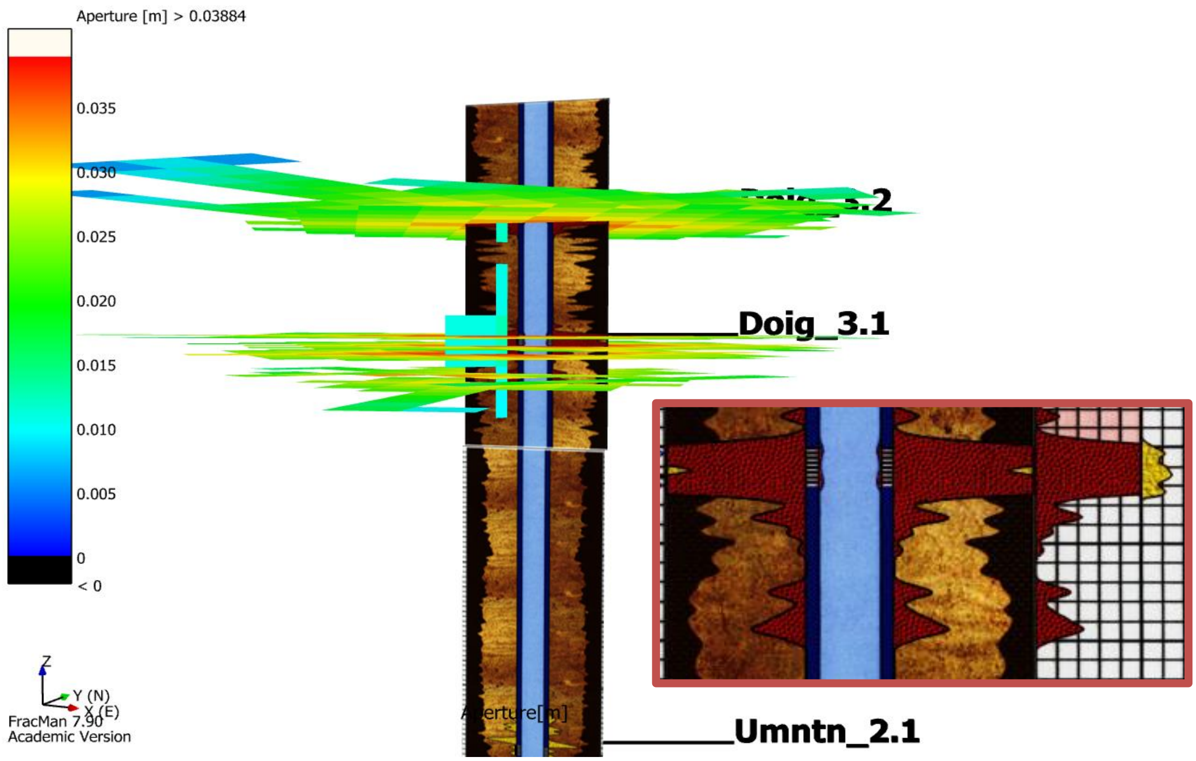

By representing bedding planes as horizontal fractures, the FracMan hydraulic fracturing

Figure 8: Doig simulated Induced fractures and inflated bedding planes. Right inset shows a detailed tracer profile at the lower Doig (3.1) perforation interval. The simulation invades bedding planes below the lower perforations that are indicated by the tracer (red).

simulator was able to provide a good match to proppant tracer profiles generated by 3 hydraulic stimulations of a vertical well. All the stimulations were pumped at ISIP pressure at the perforations using the same pressure falloff function to the fracture tips. Despite higher normal stresses acting on bedding planes; the low tensile strength and lower elastic modulus in the vertical direction allowed bedding planes to dilate and take most of the fracturing fluid. Planar fracture modeling required a remarkably high leak-off and still predicted too much vertical growth as compared to the DFN approach of including bedding planes as horizontal fractures.

Vertical Well Summary

• Bedding planes play a significant role in Montney hydraulic fracture stimulations. There is evidence of bedding plane slip in core, casing deformation measurements, and proppant tracing in vertical wells. This can be captured and estimated in hydraulic fracturing models that include bedding planes.

• Best efforts to match vertical tracer extents with simple planar fractures requires most of the injected fluid to be lost to leak-off. This results in gross underestimation of fracture surface area and fracture growth distance from the well.

• Optimization of pad, well and fracture design will be compromised by a planar fracturing model. Models that included bedding planes suggest that well spacing could be twice that estimated by models that use only induced planar fractures.

Laying Down the Full Montney

For the vertical well, bedding planes were placed at depths corresponding to the proppant tracer peaks. For a well pad model of horizontal wells without proppant tracer logs, a statistical approach is needed. Several types of vertical logs are compared in Figure 9 to determine the appropriate bedding intensity needed for the DFN model.

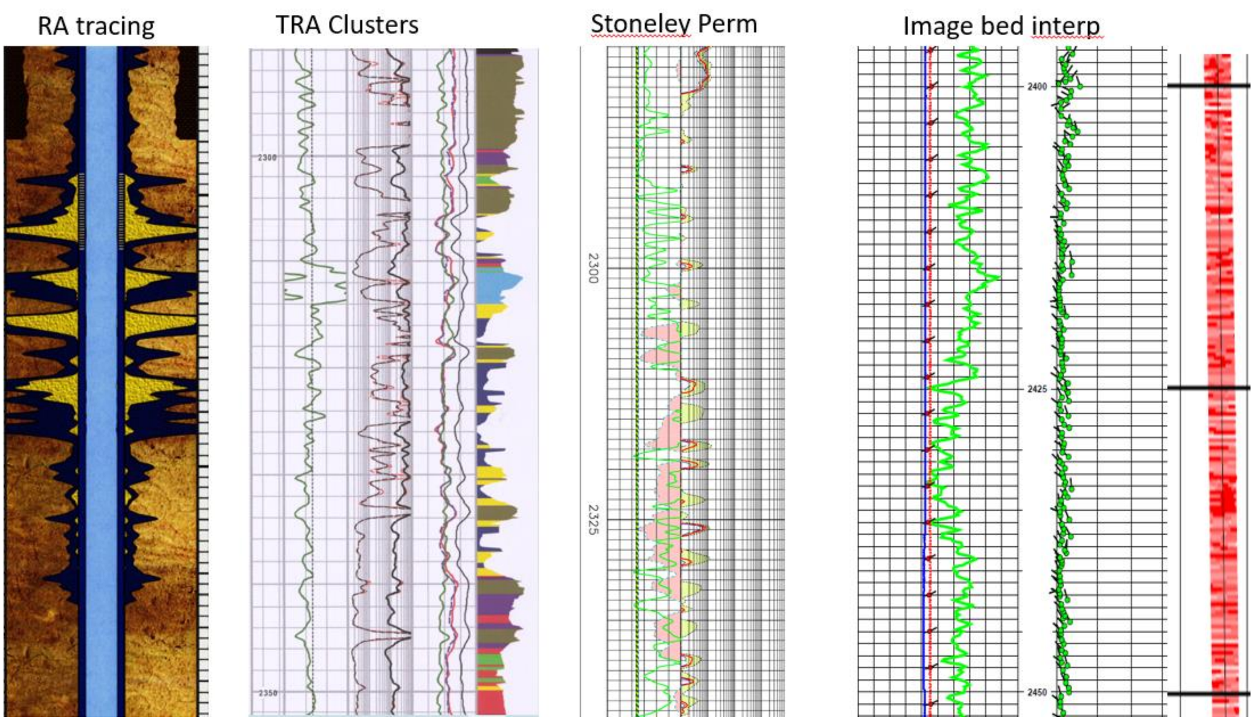

Figure 9: Logs taken from various vertical wells. Comparison with the tracer log suggests that mechanical boundaries represented by Tight Rock Analysis (TRA) Clusters and the red and yellow peaks of the Stoneley Permeability log are good indicators of beds that may take fracturing fluid. The image log to the right has a higher intensity of bedding interpreted and would require additional analysis to filter it down to fewer beds.

An active bed intensity of 0.5 beds/m was chosen after examination of the tracer, TRA cluster and Stoneley Permeability logs. The model was populated with beds oriented parallel to the model layers. Bed intersections with the vertical well and a horizontal well are shown in Figure 10. The inset shows that the active bedding intensity (green) is like the propped beds (yellow) near the perforated intervals. The modeled horizontal well has a similar bed intersection intensity in the nearly vertical section and sparse intersections along the horizontal lateral. This suggests that few stages are likely to directly pump into a bedding plane. The stress concentrations at the wellbore wall in this strike slip regime could generate short drilling-induced-tensile fractures but they are unlikely to extend out of the reduced stress zone near the wellbore during hydraulic fracturing.

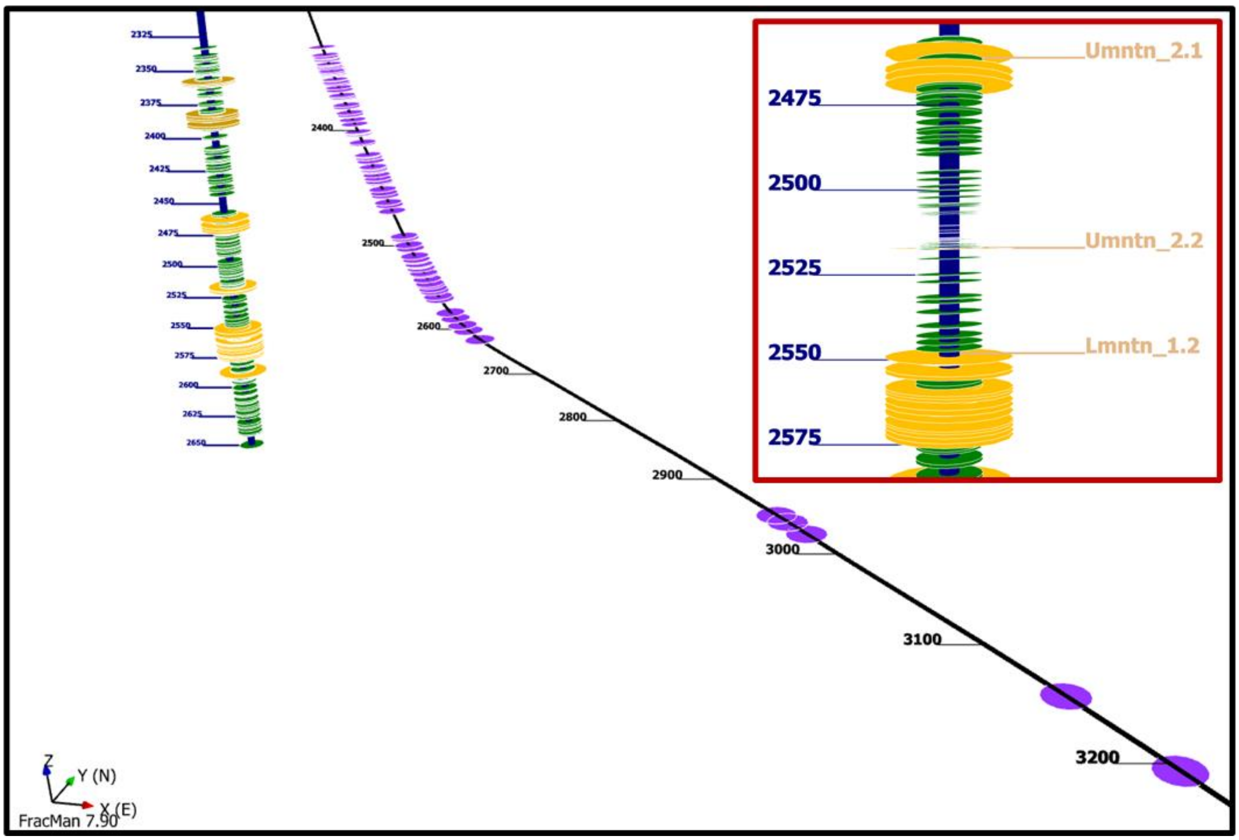

Figure 10: Intersections with the beds in the DFN model are shown in green and purple for the vertical and horizontal well. The yellow discs represent the RA tracer peaks that represent invaded beds near the perforations indicated by the labels in the inset.

Examination of several image logs in the area revealed that a fracture zone was intersected by a well at an adjacent well pad (Figure 11). Eleven fractures were intersected over 45 m in the build section of the well. They are visible on both electrical and acoustic image logs suggesting a conductive fluid present in the fracture and an open aperture that does not reflect the sonic wave.

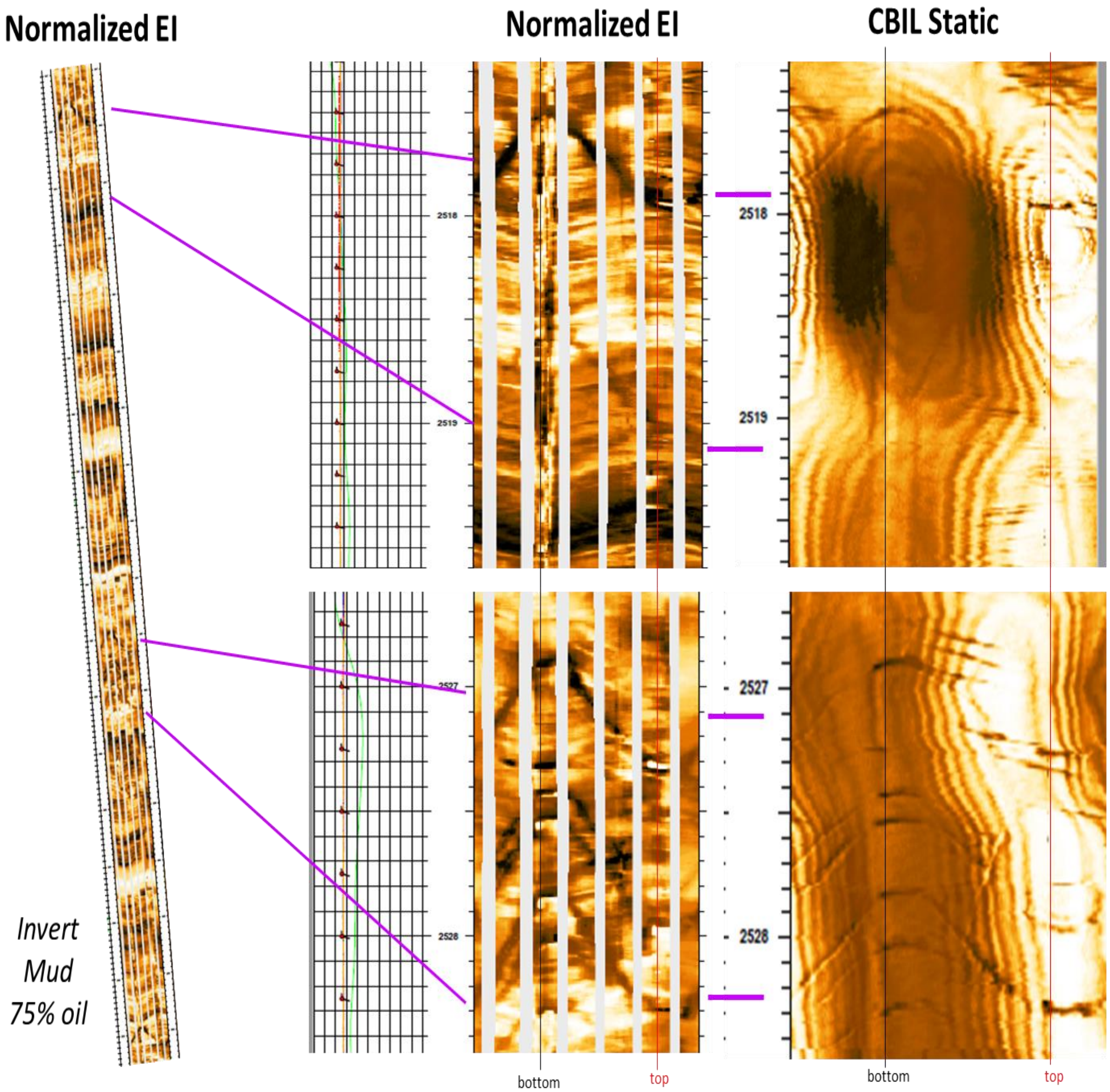

Figure 11: A 45 m Electrical Image (EI), interval EI and CBIL views of two, 2 m intervals showing 6 NW dipping open fractures. The dark band along the acoustic (CBIL) images is caused by the pipe grooving on the bottom of the hole.

Figure 12 shows that the fracture zone was located between two faults interpreted from the image log. The upper fault has associated bedding dips up to 47°, and the lower fault appears as an abrupt contact between low resistivity (dark) and resistive beds with an associated high Gamma Ray peak of 645 API. Bed dips increase by 10°across the contact.

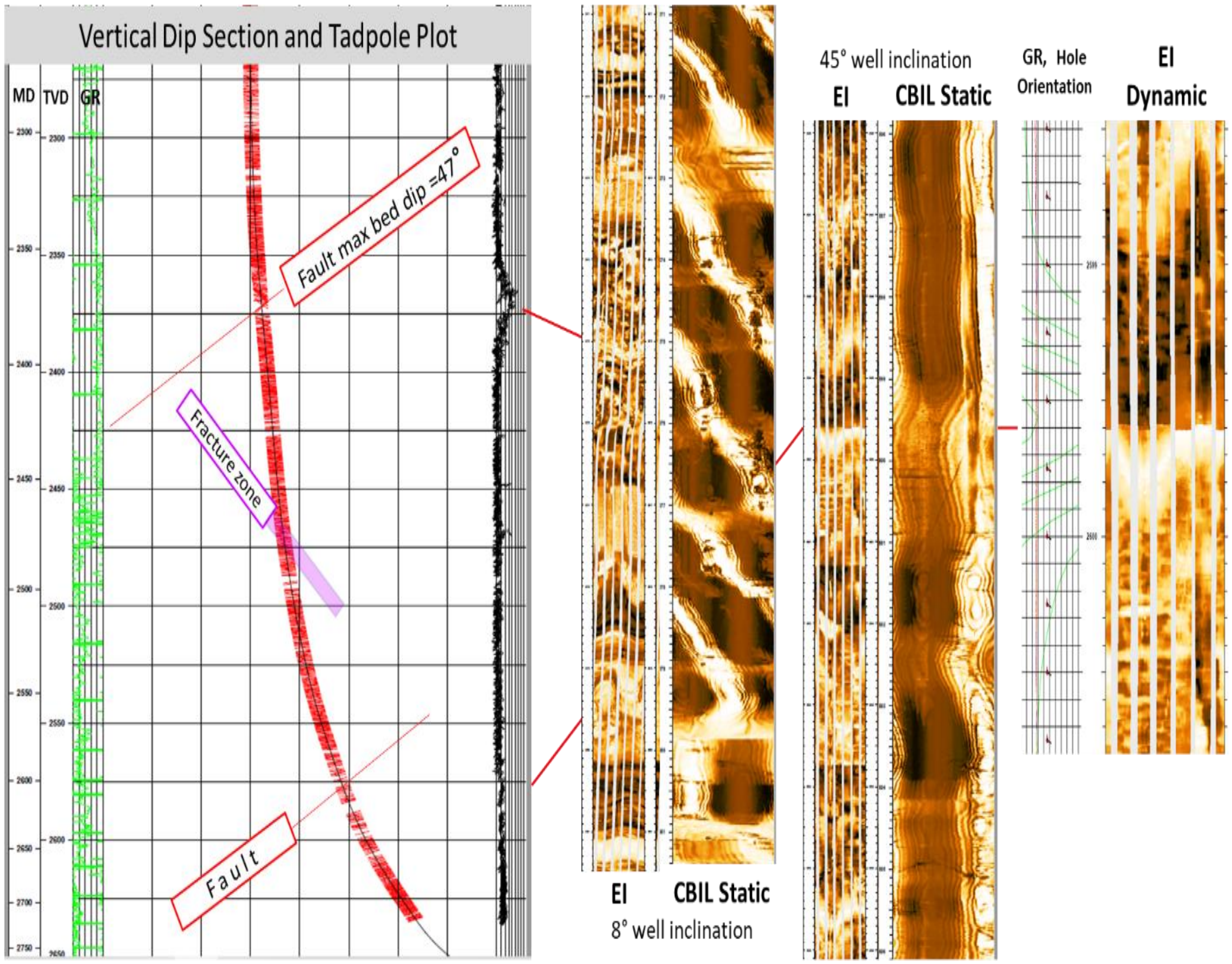

Figure 12: Vertical section of bedding dip with the Figure 3 fracture zone between two interpreted faults. Note the acoustic amplitude variation spirals in the near vertical sections the bottom of hole pipe groove is the least amplitude in the more steeply inclined hole.

Natural fractures are an important element for a horizontal well pad model. Although natural fractures were added to the vertical well analysis, they had little effect on the simulated hydraulic fracturing. By themselves vertical image logs have a low probability of intersecting the less abundant larger fractures that are needed for modeling. These larger fractures may be fault and fold associated so seismic derived attributes like curvature and discontinuity can be used to guide natural fracture distribution. Interpreted faults can be represented either as planes or planar zones of high fracture intensity. In the Montney some fracture zones may occur at the upper tip-out zone of deeper faults. Gas kicks can be another indicator of faults, large fractures, and bedding planes that act as glide planes to thrust faulting (Figure 13).

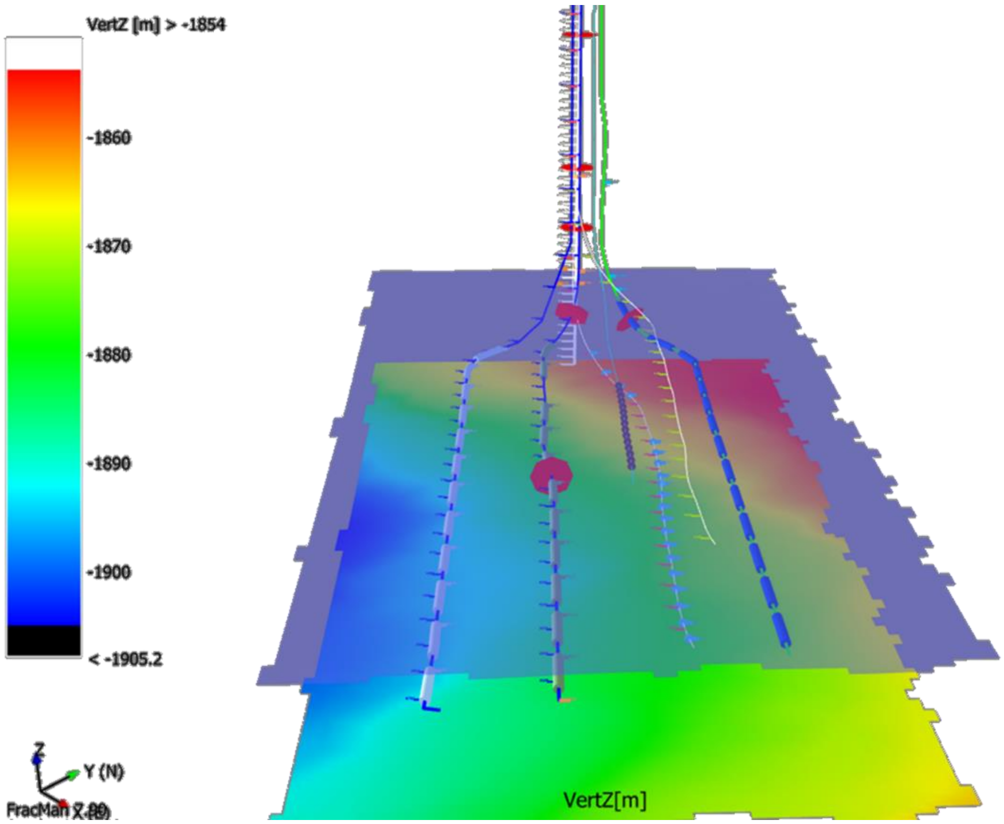

Figure 13: *Montney base structure (coloured) Montney top (transparent navy) and gas kicks (red discs). Gas kicks occur in bedding planes above and within the Upper Montney. The uppermost laterals are spaced at ~210 m.*

Micro-seismic monitoring in the area suggests that natural fracturing and faulting impact most fracturing stages. As micro-seismic data was not available for the studied pad, the published results of Rogers, McLellan and Webb (2014), and Davey (2012) were used to build a natural fracture model. The vertical fracture sets were assigned the intensity suggested by Rogers and McLellan and the ratio of the major NE striking fractures to SW striking fractures from Davey was used (Figures 14 & 15). The incidence of large natural fracture intersection in vertical wells was used to validate and adjust the natural fracture orientation dispersion (Figure 16). As orientation dispersion increases, more fractures deviate from vertical, increasing the likelihood that they will be intersected by vertical wells.

- Natural fractures are generated in 3 regions based on fracture intensity in the C085 image and consideration of elastic layers
- Fractures in the upper and middle regions are clipped to bounding surfaces
- The Lower Montney fractures are not clipped so some extend into the middle layer as suggested in Rogers and McLellan (2014).

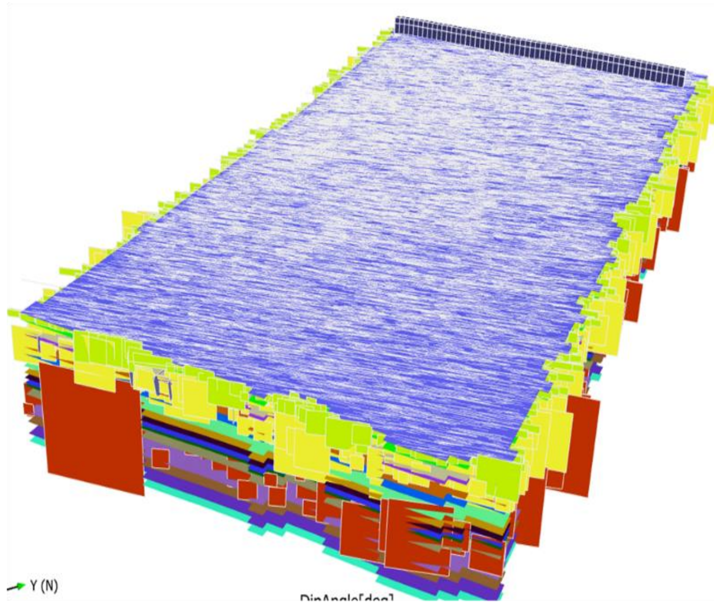

Figure 14: 3D View of the Montney well pad DFN model. White fracture traces on the Montney top surface illustrate the highest fracture intensity. The far row of grid cells shows the 2 layers above the Montney. The DFN model is about 1200 x 2400 in area by 246m i in area by 246m in thickness. Not shown are the bedding planes that occupy the entire model thickness.

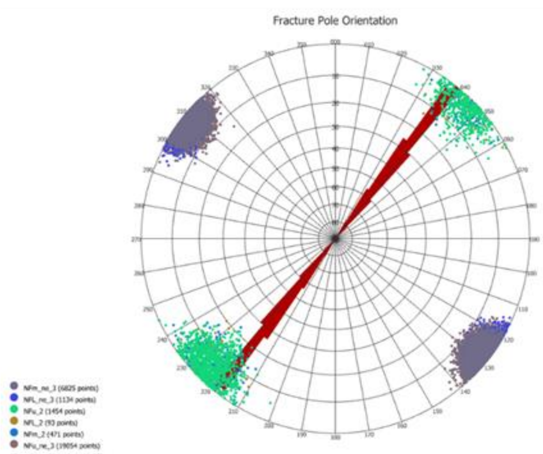

- Scaled vertical C085I imaged fracture intensity- NW striking vertical fractures
- Fault zone fractures from deviated C065I image (not shown in plot)
- Davey analysis of orientation,
  - 65% NE, 5% NW
- Rogers intensity scaling from Microseismic, faults from curvature
- Model 4: NE fractures assumed to be vertical, low dispersion k=300

Figure 15: Stereonet plot of the poles to the fractures in 3 NE striking and 3 NW striking sets. The rose plot in red shows the dominant NE sets in 2 ° bins. For the NW sets mostly the upper zone poles are visible in green.

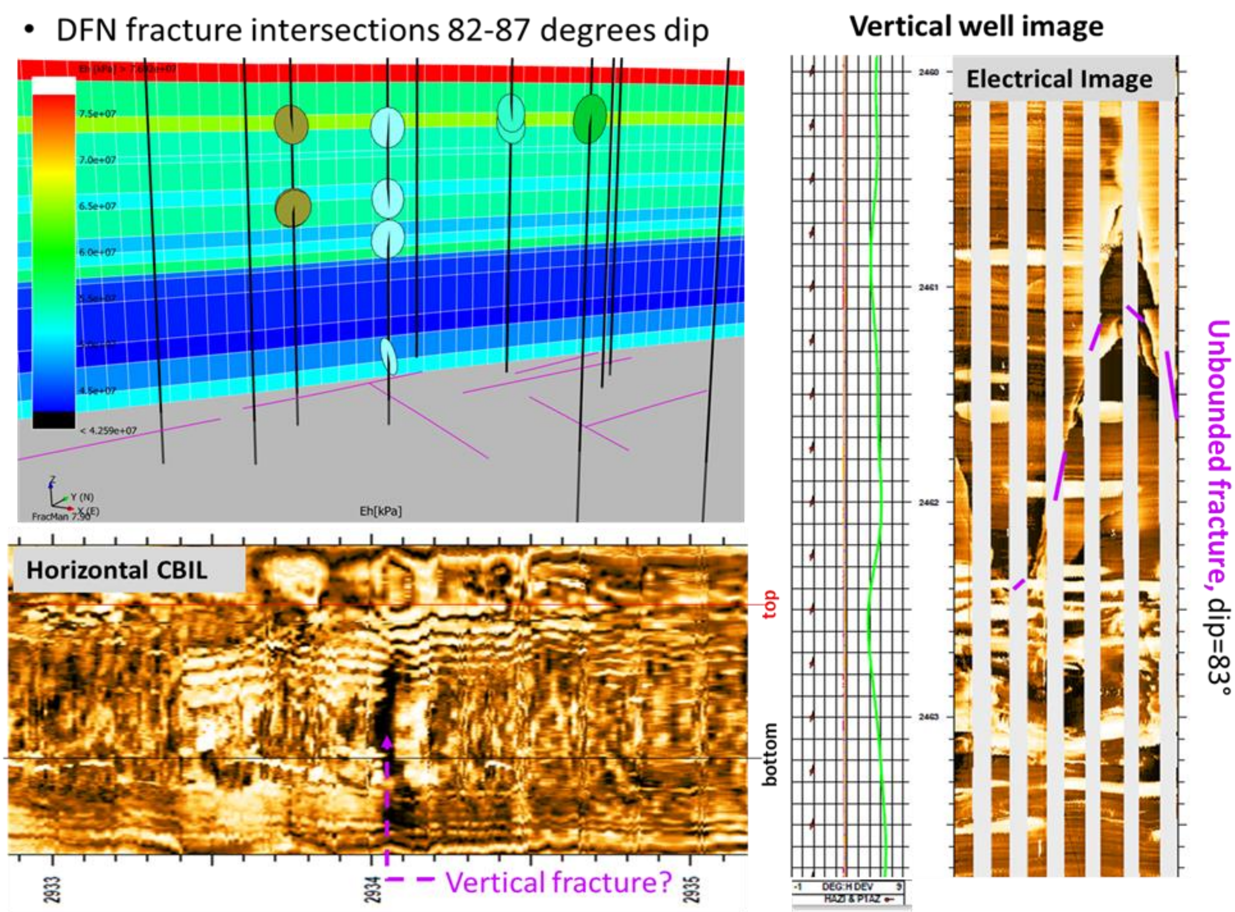

Figure 16: DFN model validation. The minority of image logged vertical wells in the area were able to image large-aperture vertical fractures. The low dispersion DFN model was able to match this when probed by 10 vertical wells. The fracture intersections are represented by disks showing the fracture orientation. Only 2 wells intersected fractures in the middle and lower fracture layers. The grid slice in the background shows the horizontal stiffness of the Montney model layers with the highest stiffness in the Doig in red and the lowest stiffness in the Lower Montney in blue. Fracture traces on the base of the Montney reflect the lower fracture intensity of the lower Montney. The vertical electrical image shows an unbounded fracture that crosses the entire image. A vertical fracture interpreted in the horizontal acoustic image is made visible by chipping out at the bottom of the hole during pipe/bit movement during connections or tripping (broad black, non-reflecting band).

In addition to the widespread natural fractures, a normal fault zone was added to the model and populated with fractures of the same orientation. From gas kicks alone it is difficult to interpret the orientation of faults. Figure 17 shows possible fault interpretations from gas kicks at the heels of wells on the modeled well pad. For modeling purposes, a normal fault zone was added to gauge the impact of inclined fractures on the hydraulic fracture modeling (Figure 18).

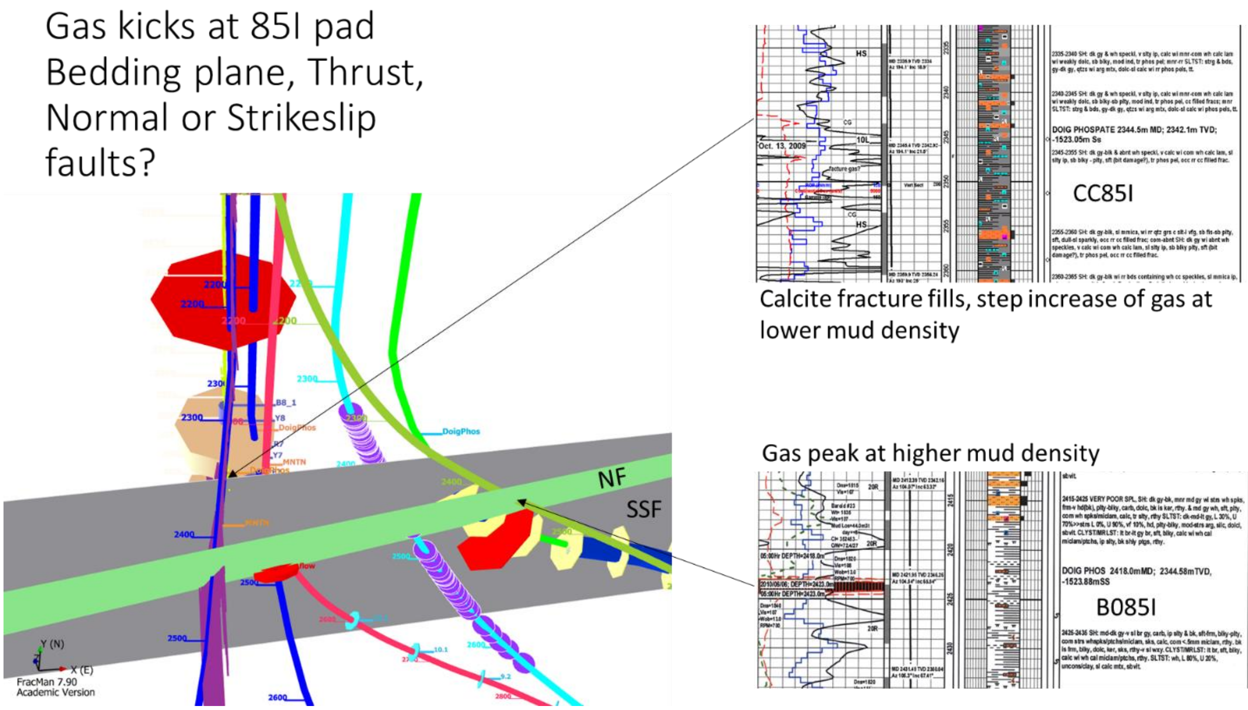

Figure 17: Possible normal fault (NF) and strike-slip (SSF) interpretations are shown for two gas kicks that occur in different stratigraphic intervals. The gas kick above those occurs at a stratigraphic contact that has gas kicks in other wells, likely a thrust fault glide plane. The geologic strip logs at the CC85I and the B085I well show gas kick examples of a step increase and an extreme gas peak.

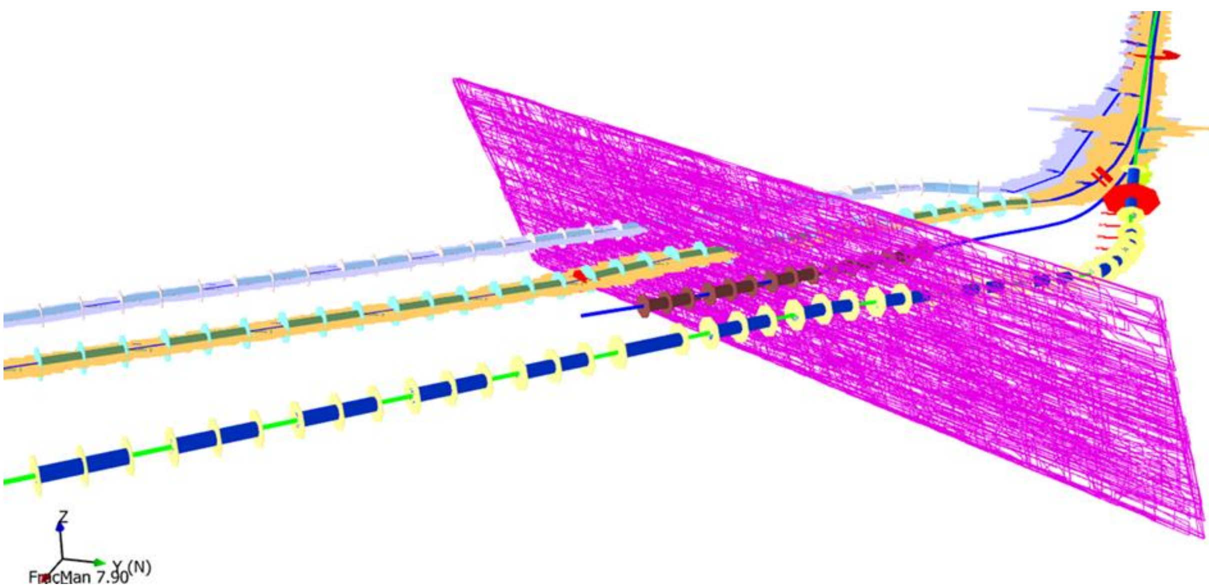

Figure 18: A view of the inserted normal fault zone crossing wells with stages represented as cylinders and perf intervals that appear as disks. The two far wells also show the GR logs acquired while drilling.

Hydraulic fracturing was simulated in the DFN model to see the effect of the natural fractures and the normal fault zone. In the CA well 5 stages were run with a stage length of 120 m and 3 perforation clusters spaced 40 m apart. The nominal field design of 1439 m^3 slickwater was pumped at the recorded ISIP pressures. Proppant concentration was ramped up in steps to a maximum of 250 kg/m^3 starting with 150 T of 40/70 sand and finishing with 10 T of 20/40 proppant.

Figure 19 shows the variation in the simulated microseismic results. Stages 1 and 2 are dominated by invasion of bedding planes via the induced fractures. Stages 3 and 4 are strongly influenced by the normal fault zone at the expense of bedding plane invasion. In stage 3 the fault zone is directly connected by an induced fracture, whereas in stage 4 bedding planes connect an induced fracture to the fault zone. Stage 5 is more strongly influenced by of the middle and lower Montney natural fractures. This is likely because this stage is deeper in the Montney than the other stages.

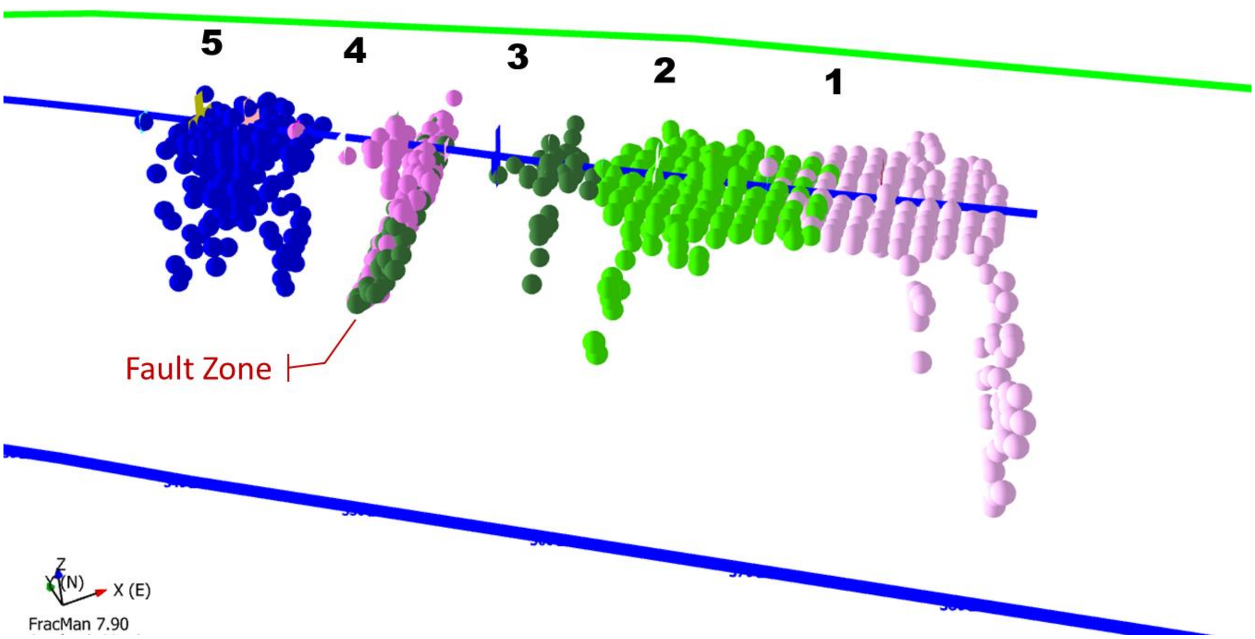

Figure 19: Simulated microseisms for 5 stages in the CA well. Note the variation and asymmetry of the results.

The instantaneous shut-in pressures (ISIP) exceed the vertical stress allowing inflation of bedding planes near the wellbore where the pore pressure is high (Figure 20). The pressure at the tips of the induced fractures falls below the vertical stress (green). The dominant NE striking fractures have the low pore pressures approaching the minimum horizontal stress.

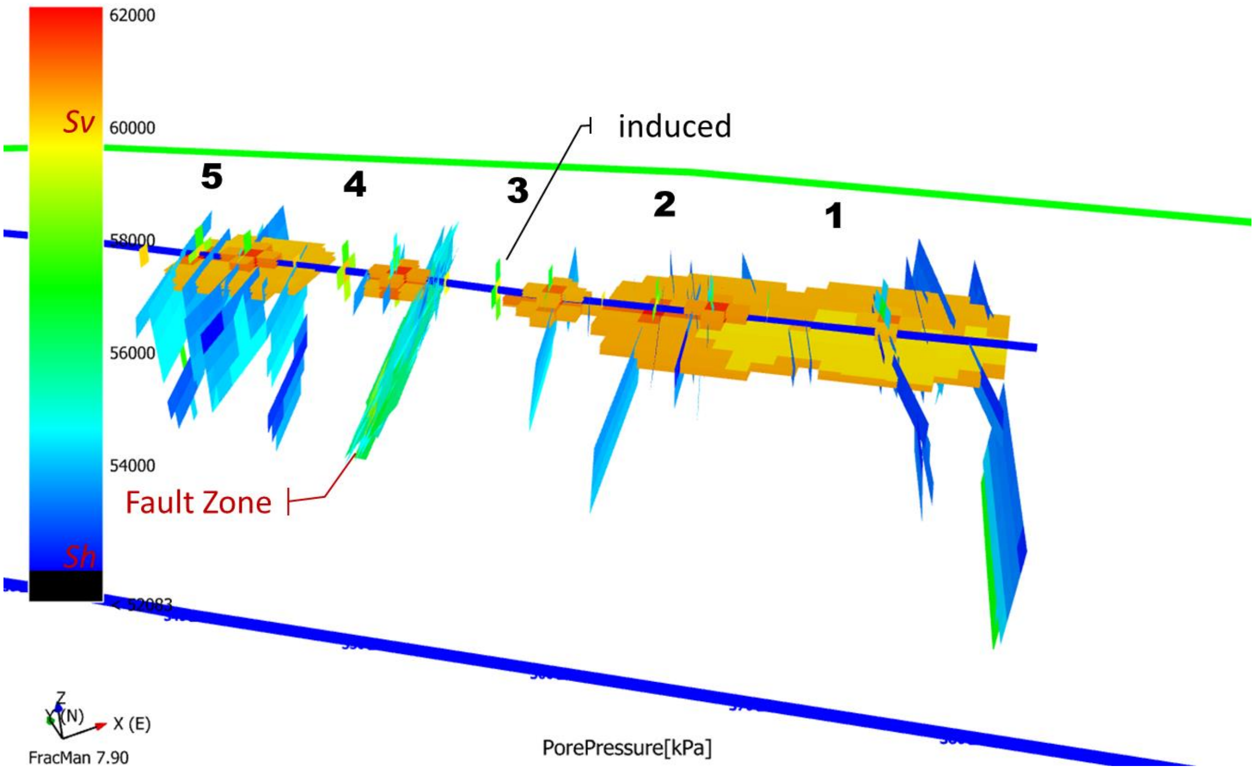

Figure 20: Fracture pore pressures decline with distance from the perforation clusters and increase with depth in response to increased gravitational head. The pore pressures of the induced and inflated fractures are limited by the normal stresses acting on the fractures.

The normal stress acting on the induced fractures, inflated fractures and inflated bedding planes are illustrated in Figure 21. The highest normal stress is acts on the bedding planes, and the lowest acts on the induced fractures. The natural fractures have normal stresses that are slightly elevated above the minimum horizontal stress depending on their deviation from a plane normal to the minimum stress. All stresses generally increase with depth in response to increased overburden load. The variations in horizontal stiffness (see Figure 16) cause a decrease in normal stress in the lower part of the inflated natural fractures in stage 5 and significantly elevate the stress at the bottom of the long natural fracture in stage 1.

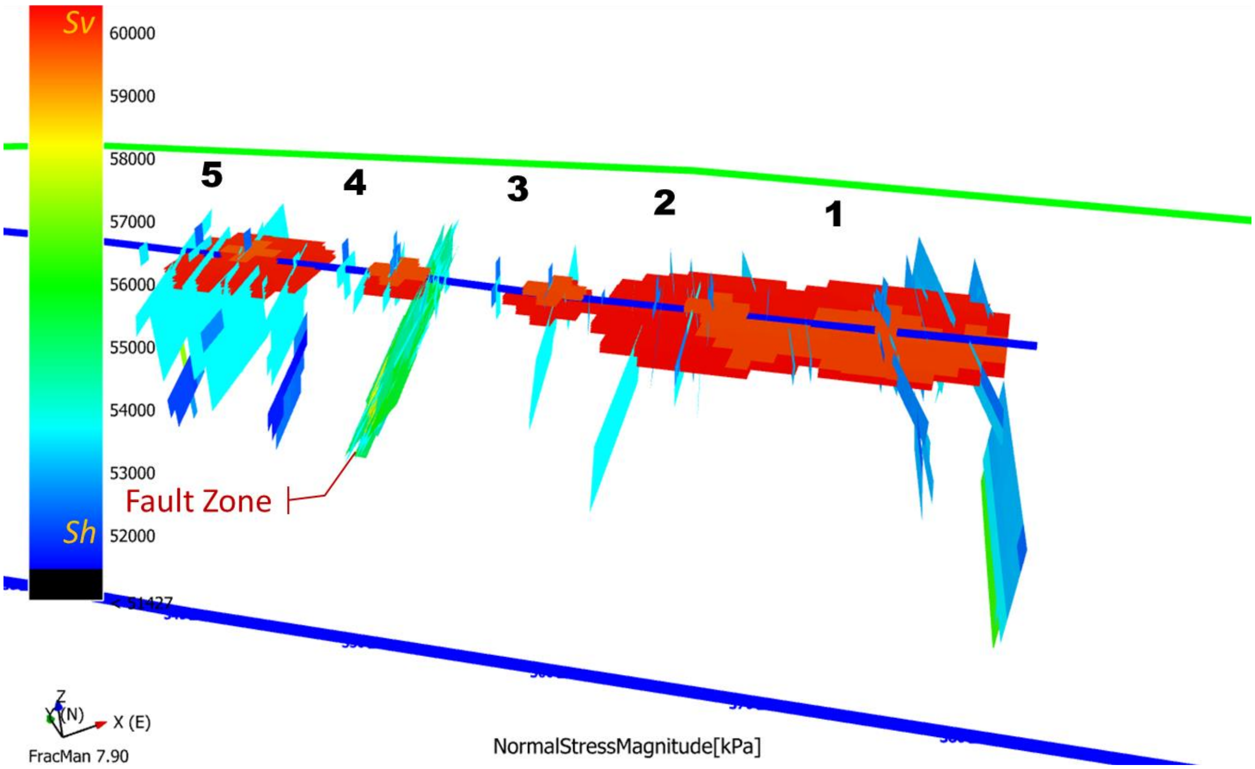

Figure 21: Normal stress acting on the fractures and bedding planes. The vertical stress (Sv) acts on the bedding planes and the minimum horizontal stress (Sh) acts on the induced fractures.

Microseismic data from the Montney in NE British Columbia shows variability between stages. Stages in three wells were simulated using the completion parameters in Table 1.

Well	Depth in Montney (m)	Stage Length (m)	Water Volume (m3)	Proppant Mass (T) & Size (mesh)
CA	135-153	120	1381	150T 40/70, 10 T 20/40, 10 T 25/50
CC	160-194	174	1089	150T 40/70, 20 T 20/40
CD	92-130	150	1835	230T 40/70, 10 T 20/40

Table 1: Average stage length, clean water volume and proppant for the stages simulated in the three wells.

The northwest well in Figure 22 has dense clouds in several stages like the simulated stages that were dominated by bedding planes. Other stages have a varied response like the simulated stages that inflated bedding planes and natural fractures. The southeast well had responses more like the simulated stages in the deeper CC well. The simulated stages in Figure 15 have a similar vertical extent to microseismic of stages recorded in the field.

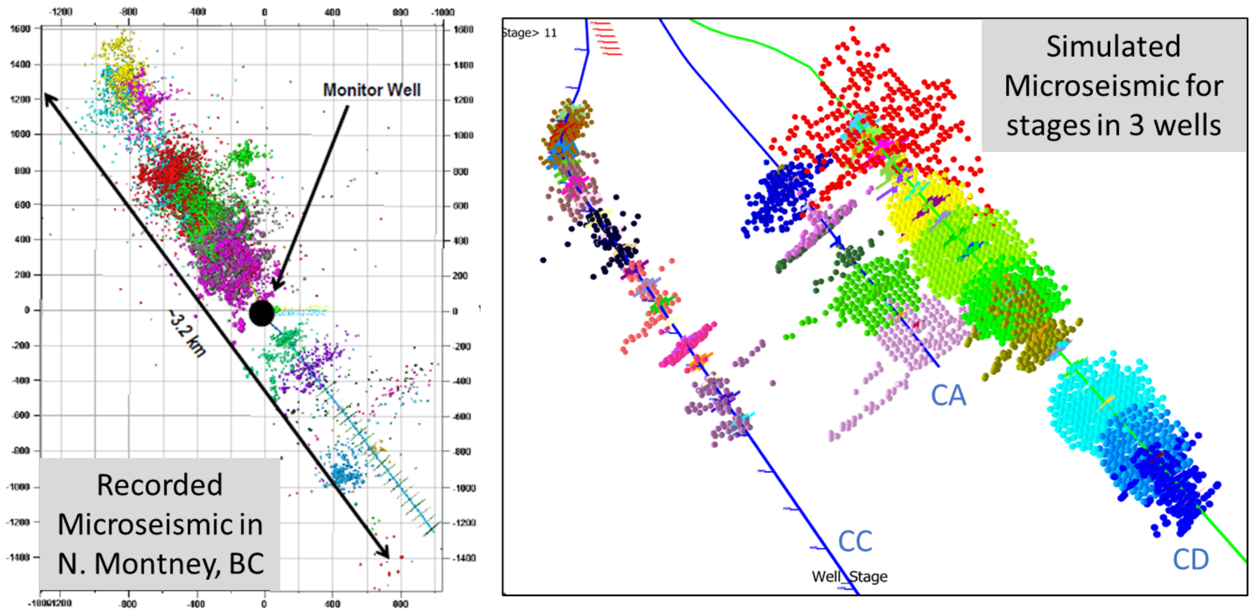

Figure 22: Map view comparison of simulated microseismic to published field microseismic (Stannard and Topolinsky, 2014).

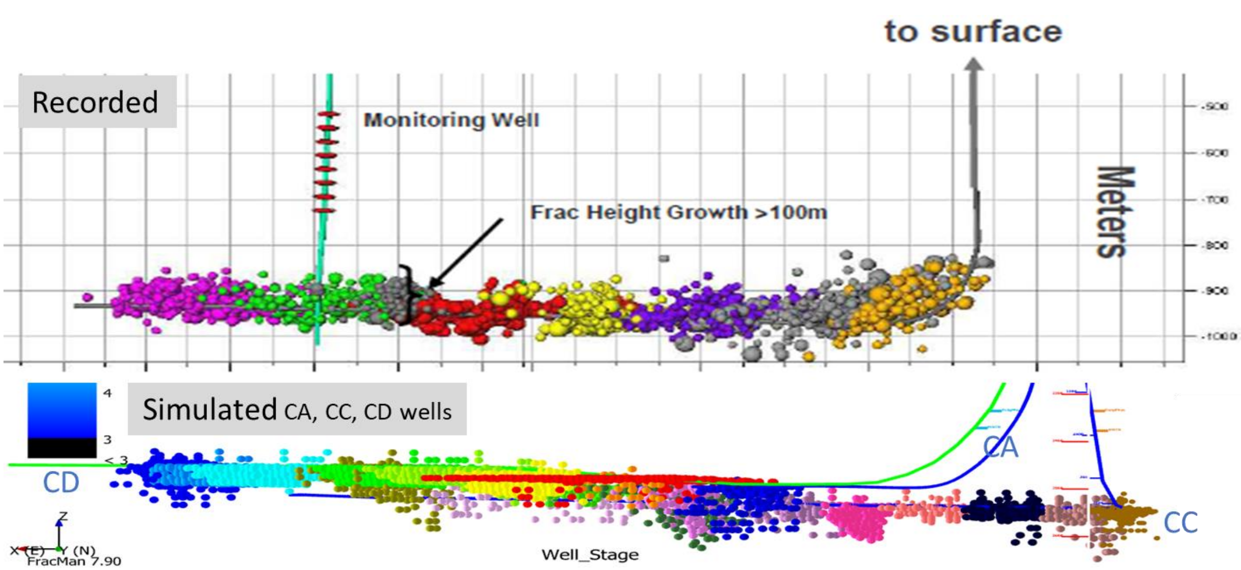

Figure 21: Cross section comparison of simulated microseismic to published field microseismic (Stannard and Topolinsky, 2014). The vertical scale is the same for both views.

Figure 24 compares the CA well simulations to microseismic data from two wells from Pouce Coupe field located to the east of the Altares field. The simulated stages have similar fracture lengths. The asymmetry in cloud half lengths is indicative of natural fracture inflation. The field example appears to have less influence of bedding planes and more dominance of natural fractures. Davey (2012) estimates a lower horizontal minimum stress in Pouce Coupe than in Altares, so pore pressures during hydraulic stimulation were less likely to exceed the vertical stress and invade bedding planes in Pouce Coupe.

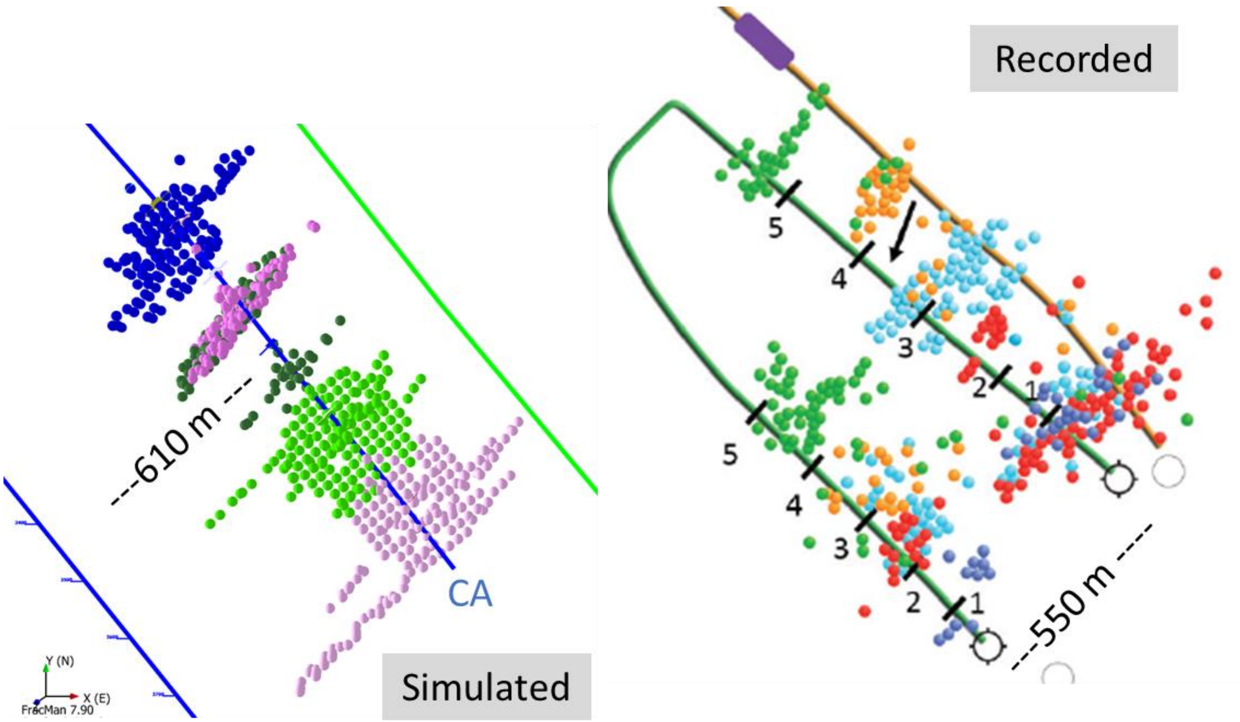

Figure 22: Map view comparing simulated stage geometries to microseismic observations published by Ouenes et al (2014).

Conclusions

Representing hydraulic fracture scenarios with simple models that ignore important geologic features can result in misleading simulation results. This paper has described several important characteristics from the Montney that impact on frac performance.

- Bedding planes play a significant role in Montney hydraulic fracture stimulations where injection pressures exceed the vertical stress. There is evidence of bedding plane slip in core, casing deformation measurements, and proppant tracing in vertical wells. This component can be readily captured and estimated in hydraulic fracturing models that include bedding planes.

- Image logs show the presence of open natural fractures but the probability of intersection of vertical fractures is low in vertical wells. Hydraulic fracture growth and fluid invasion of bedding planes increase the likelihood of injecting into natural fractures. Injection pressures are sufficient to open natural fractures that are completely cemented with calcite. Natural fractures will dominate stages where an early connection is established.
- Connection to fault zones with a high intensity of natural fractures will also dominate nearby stages. Early connection to a fault zone can prevent invasion of bedding planes.
- Natural fractures and fault zones increase the distance, asymmetry, and variability of hydraulic stimulations.
- Best efforts to match vertical tracer extents with simple induced planar fractures requires most of the injected fluid to be lost to leak-off. This results in gross underestimation of fracture surface area and fracture growth distance from the well.
- Optimization of pad, well and fracture design will be compromised by a planar fracturing model. Models that included bedding planes suggest that well spacing could be twice that estimated by models only using induced planar fractures.
- Forcing simple models to ignore important geologic features can lead to suboptimal field developments. These suboptimal developments have been repeated in many plays to the extent that data analytics have shown widespread reduced well productivity and overcapitalization.

Acknowledgements

The work was made possible by the help of Steve Rogers and Neal Josephson of Golder Associates for providing advice and a FracMan software license. The work of several graduate students was helpful in constructing the mechanical zonation, elastic, and stress models. A big thanks to Petro Ninja for providing well data access during the COVID-19 pandemic. This enabled a much more detailed analysis than would have been possible from limited data and published works.

References

Davey, H., 2012. *Geomechanical characterization of the Montney shale, northwest Alberta and northeast British Columbia Canada*. MSc.Thesis. Colorado School of Mines, Denver, Colorado

Keneti, R. 2011. *Some geomechanical properties of Montney shale.* MSc thesis. University of Calgary, Calgary, AB.

McLellan, P, 2019. Casing Shear Deformations Created in the Montney During Hydraulic Fracturing Operations: What We See, Why It Happens, and What We Can Do About It. Canadian Society for Unconventional Resources (CSUR) Montney Workshop, Calgary

Ouenes, Ahmed & Aimene, Yamina & Nairn, John. 2014. *Interpretation of Microseismic Using Geomechanical Modeling of Multiple Hydraulic Fractures Interacting with Natural Fractures – Application to Montney Shale*., CSEG Recorder, November 2014.

Rogers, S., McLellan, P., Webb, G., 2014. *Investigation of the Effects of Natural Fractures and Faults on Hydraulic Fracturing in the Montney Formation, Farrell Creek Gas Field, British Columbia*, DFNE 2014 - 224, Vancouver, BC, October, 2014.

Song, L. 2012. *Measurement of minimum horizontal stress from logging and drilling data in unconventional oil and gas* MSc Thesis. University of Calgary, Calgary, AB

Stannard, J. & Topolinsky, D., 2014. *The North Montney*. https://apps.cer-rec.gc.ca/REGDOCS/File/Download/2541375